Correcting strain Measurements of Strain-Encoding (SENC) MRI with Slice Following

T. A. Yousef[1,2], and N. F. Osman[1,2]

[1]ECE Dept., Johns Hopkins University, Baltimore, MD, United States, [2]Department of Radiology, Johns Hopkins University, Baltimore, MD, United States

Introduction: Strain Encoding (SENC) Imaging technique has shown the ability to detect through plane tissue deformations. The slice following technique is used in applications of cardiac MRI in order to image the same slice throughout the cardiac cycle. In this work, a thorough analysis is presented to address the effect of using slice following with SENC imaging technique and the accuracy of the resulting measurements.

Theory: In SENC, The acquired images are modified by adding a gradient moment in the slice-selection direction to cause demodulation with a specific spatial frequency, which is called the *tuning* frequency. Two Images I_L and I_H are acquired for two different tuning frequencies ω_L, ω_H in order to be able to calculate the frequency peak shift and then estimating the longitudinal strain [1]. Given the targets minimum and maximum strain values ($\varepsilon_{\min}, \varepsilon_{\max}$), the tagging and tuning frequencies can be calculated as in [2]. The main idea is to guarantee that there is a signal at the two tuning frequencies through the whole range of frequency shifts caused by tissue deformations. In addition, the low tune frequency must not interfere with the DC component of the signal. These calculations depend on the assumption that the width of the harmonic peak (B) is constant through time. Where B is directly related to slice thickness, and in case of rectangular slice profile B=1/slice Thickness. However, because of using slice following, the harmonic peak width and magnitude change due to tissue deformation (fig. 1). This results in changes in selecting the SENC imaging parameters and computations.

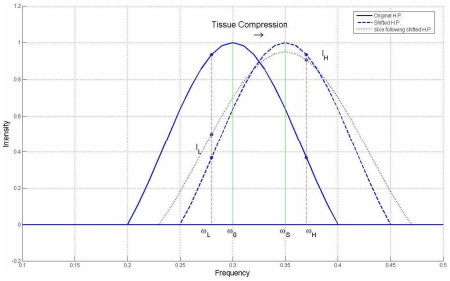

Fig. 1: Harmonic peak shift for the the normal and slice following imaging. Note that for compression, the peak of slice following becomes wider (thinner slice) and its magnitude is decreased (to preserve constant area under the curve.)

Change 1) Selection of SENC parameters (tagging frequency ω_0, low and high tune frequencies ω_L, ω_H):

For a given slice thickness (B_0) before deformation and arbitrary strain (ε_t), the new profile width is given by

$$B_t = B_0 / (1 + \varepsilon_t). \qquad (1)$$

Therefore, the constraint conditions in [2] can be re-written as:

1. In order not to interfere with the DC component, $\omega_L \geq B_{\max} \Rightarrow \omega_L \geq B_0 / (1 + \varepsilon_{\max})$, (2)
2. To guarantee that the tuning frequencies are always within the peak range, $(\omega_H - \omega_L)_t \leq B_t$, (3)

where ω_L and ω_H are related to $\varepsilon_{\min}$ and $\varepsilon_{\max}$ as $\varepsilon_{\min} = (\omega_0 / \omega_L) - 1$ and $\varepsilon_{\max} = (\omega_0 / \omega_H) - 1$.

Since the relation between the tuning frequencies becomes time dependant, it is hard to obtain a closed form for the tagging and tuning frequencies given the required strain range and initial slice thickness. Therefore, an iterative algorithm was developed in order to get the solution.

Change 2) Computation of the strain:

Due to the changing width of the harmonic peak—due to local strain, the resulting strain values resulting from [1] are largely affected. In order to correct for this error, the initial estimate of the shifted frequency ($\bar{\omega}_s$) is used to calculate a scaling factor for both I_L and I_H to compensate for the peak width variations as follow:

$$f_t = \mathrm{sinc}\left((\omega_L - \bar{\omega}_s)/B_0\right) / \mathrm{sinc}\left((\omega_L - \bar{\omega}_s)/\bar{B}_t\right), \qquad (4)$$

Where $\bar{B}_t$ is calculated using (1) and the initial estimate stain value $\bar{\varepsilon}_t$. A similar factor can also be calculated for the high tuning. Plug f_t in the strain calculation to obtain a better estimate for the strain value (Fig. 2 and 3).

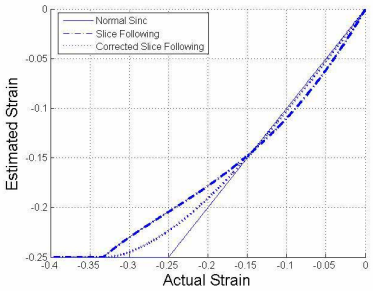

Fig. 2: Estimated strain vs. actual strain for the normal, slice following and correct slice following SENC calculations.

Change 3) Effect on the Anatomy Images (Magnitude Values):

Since the spins density in the excited slice is constant, the area under the slice profile is also constant. Therefore, tissue deformation does not only affect the width of the harmonic peak, but the height of this peak as well. While this does not affect the strain values (see the strain Eq. in [1]), it can largely affect the anatomy image constructed from I_L and I_H. In order to correct for that, another scaling factor (g_t) is introduced to compensate for intensity changes. In contrast to f_t , g_t will be the same for both I_L and I_H. g_t is calculated as follows:

$$g_t = \frac{A_0}{A_t}, \text{ where } A_0 = \int_{-B_0/2}^{B_0/2} \mathrm{sinc}\left(\frac{b}{B_0}\right) db \text{ and } A_t = \int_{-B_t/2}^{B_t/2} \mathrm{sinc}\left(\frac{b}{B_t}\right) db,$$

which by simple algebra and using (1), the last equation can be simplified into

$$g_t = (1 + \varepsilon_t), \qquad (5)$$

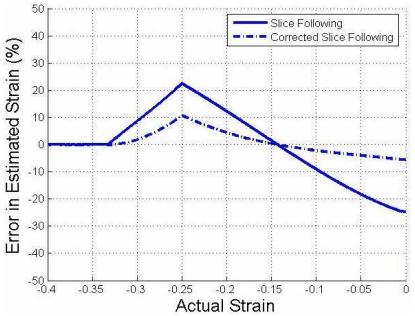

Fig. 3: Error in estimated strain for slice following SENC and the correction algorithm.

Methods: First, iterative algorithm was developed in order to determine ω_0, ω_L and ω_H for given B_0, $\varepsilon_{\min}$ and $\varepsilon_{\max}$:

1. Let $\omega_{L_i} = B_0 / (1 + \varepsilon_{\max})$ to guarantee avoiding the interference with the DC component in its max width.
2. Given ω_{L_i}, compute $\omega_{0_i} = \omega_{L_i}(1 + \varepsilon_{\min})$, then given ω_{0_i}, compute $\omega_{H_i} = \omega_{0_i} / (1 + \varepsilon_{\max})$
3. If $\omega_{H_i} - \omega_{L_i} \geq B_0 / (1 + \varepsilon_{\max})$ stop.
4. Let $\omega_{L_{i+1}} = \omega_{L_i} + \Delta$, where Δ a small frequency shift, then goto step 2.

Second, numerical simulation for the effect of peak width variation on the magnitude is built. Rectangular slice profile was assumed with initial width, then changing this width step by step, calculating the actual strain and the measured strain using SENC. The same simulation is repeated with introducing the scaling factor f_t to I_L and I_H before calculating the estimated strain.

Results: Fig. 2 shows the simulation result for the effect of slice following on the strain measurements (over a selected strain range) using SENC. Note that the strain range in slice following (the dashed line) is wider. However, its values have either an over- or under-estimation for the strain values. The dotted line shows the corrected values using the proposed algorithm. Fig. 3 shows the errors in strain values for the SENC calculations in slice following with and without the correction algorithm. It shows that the maximum error in strain values is 10% for -25% strain values which means an overall error of at most 2.5% in the estimated values.

Conclusion: A detailed analysis of the effect of slice following imaging on SENC technique was discussed. An iterative algorithm for parameters selection for the SENC was introduced. Two correction algorithms for strain computations and pixel intensities are proposed for obtaining more accurate strain maps and better anatomy images, respectively.

References: [1] Nael F. Osman, "Imaging longitudinal cardiac strain on short-axis images using strain-encoded MRI," Magn. Resn. Med. 46: 324-10 (2001).
[2] Tamer Yousef et al., "The effect of noise on the accuracy of strain measurment when using strain encoded (SENC) MRI," Proc ISMRM 2006, #1658.